

Probing Electron Correlation via Attosecond XUV Pulses in the Two-Photon Double Ionization of Helium

J. Feist,^{1,*} S. Nagele,¹ R. Pazourek,¹ E. Persson,¹ B. I. Schneider,^{2,3} L. A. Collins,⁴ and J. Burgdörfer¹

¹*Institute for Theoretical Physics, Vienna University of Technology, 1040 Vienna, Austria, EU*

²*Physics Division, National Science Foundation, Arlington, Virginia 22230, USA*

³*Electron and Atomic Physics Division, National Institute of Standards and Technology, Gaithersburg, Maryland 20899, USA*

⁴*Theoretical Division, T-4, Los Alamos National Laboratory, Los Alamos, New Mexico 87545, USA*

(Dated: June 18, 2021)

Recent experimental developments of high-intensity, short-pulse XUV light sources are enhancing our ability to study electron-electron correlations. We perform time-dependent calculations to investigate the so-called “sequential” regime ($\hbar\omega > 54.4\text{ eV}$) in the two-photon double ionization of helium. We show that attosecond pulses allow to induce and probe angular and energy correlations of the emitted electrons. The final momentum distribution reveals regions dominated by the Wannier ridge break-up scenario and by post-collision interaction.

PACS numbers: 32.80.Rm, 31.15.V-, 32.80.Fb, 42.50.Hz

Understanding the role of electron correlation in atoms, molecules, and solids has been a central theme in physics and chemistry since the early days of quantum mechanics. Most of the focus has centered on the role of electron correlation in (quasi-)stationary states. Recent progress in the development of light sources provides unprecedented opportunities to expand our understanding of electron correlation to dynamical processes where external fields play a critical role. The availability of attosecond pulses, as generated from high-harmonic radiation [1–3], opens new avenues for time-domain studies of multi-electron dynamics. Using such pulses, it is possible to not only observe, but also actively *induce* and *control* correlation effects.

The simplest system where electron-electron interaction can be studied is the helium atom. Unraveling the intricacies of electron correlation in ultrashort and intense electromagnetic fields interacting with this simple atom is critical to our understanding of the same processes in more complex systems. Despite the computational challenges, the dynamics of He under the influence of external fields can still be accurately simulated in *ab initio* calculations, cf. [4]. The results of the present investigation provide evidence that the effects of electron correlation can be surprisingly complex in situations dominated by external ultrashort fields. This in turn has important consequences for attosecond studies in molecules, clusters, and solids. We show that it is possible to disentangle the different processes occurring in such pulses by analyzing the final momentum distribution of the ejected electrons.

Double ionization of helium by single photon absorption has long been the benchmark for our understanding of correlation effects in the three-body Coulomb problem [5–9]. The availability of intense light sources in the VUV and XUV region [10–12] has recently shifted attention from single-photon double ionization and intense-IR laser ionization by rescattering (see [13–15] and references

therein) to multiphoton ionization. Restricting attention to only two-photon double ionization (TPDI) enables us to distinguish two spectral regions. The “nonsequential” or “direct” regime between $39.5\text{ eV} < \hbar\omega < 54.4\text{ eV}$ has recently received considerable attention (see [16–21] and references therein). Energy-sharing between the electrons, and thus correlations, are a *conditio sine qua non* for double ionization to occur in this regime. By contrast, in “sequential” TPDI with $\hbar\omega > 54.4\text{ eV}$ [22–25], each photon has sufficient energy to ionize one electron within an independent-particle model and electron-electron interaction, while present, is not a necessary prerequisite.

For an ultrashort pulse of attosecond duration the concept of “sequential interactions”, valid for long pulses, becomes obsolete. Instead, the two-electron emission occurs almost simultaneously, and the strength of electron correlation in the exit channel can be tuned by the pulse duration T_p . This information is encoded in the final joint momentum distribution $P(\mathbf{k}_1, \mathbf{k}_2) \equiv P(E_1, E_2, \Omega_1, \Omega_2)$, experimentally accessible in kinematically complete COLTRIMS measurements [26].

In our current calculations we solve the time-dependent Schrödinger equation in its full dimensionality, including all inter-particle interactions. The laser field is linearly polarized and treated in dipole approximation. The duration T_p is given by the FWHM of a sine-squared envelope function for the electromagnetic field. The computational approach is based on a time-dependent close-coupling (TDCC) scheme where the angular variables are expanded in coupled spherical harmonics and the two radial variables are discretized via a finite element discrete variable representation (FEDVR). Temporal propagation is performed by the short iterative Lanczos (SIL) algorithm with adaptive time-step control. The asymptotic momentum distribution is obtained by projecting the wave packet onto products of Coulomb continuum states. Projection errors due to the replacement of the full three-body final state by independent-particle Coulomb wave

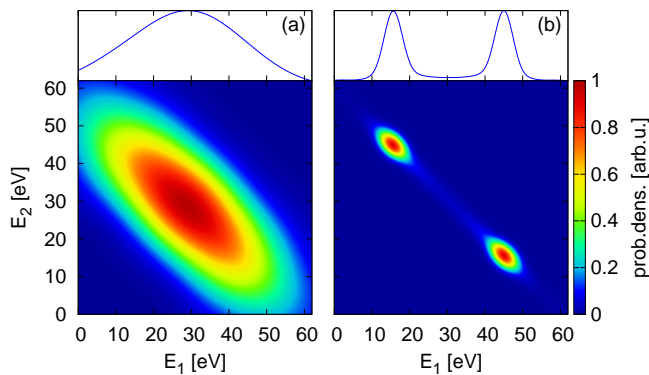


FIG. 1: TPDI electron spectra $P(E_1, E_2)$ at $\hbar\omega = 70$ eV for different pulse durations (FWHM): (a) $T_p = 150$ as, (b) $T_p = 750$ as. The top shows the spectrum integrated over one energy, i.e., the one-electron energy spectrum $P(E_1) = P(E_2)$.

functions can be reduced to the one-percent level by delaying the time of projection until the two electrons are sufficiently far apart from each other [19].

The joint energy probability distribution

$$P(E_1, E_2) = \iint P(E_1, E_2, \Omega_1, \Omega_2) d\Omega_1 d\Omega_2 \quad (1)$$

reveals the breakdown of the sequential ionization picture with decreasing pulse duration T_p (Fig. 1). For long pulses, two distinct peaks signifying the emission of the “first” electron with energy $E_1 = \hbar\omega - I_1$ (with $I_1 = 24.6$ eV the first ionization potential) and the “second” electron with $E_2 = \hbar\omega - I_2$ ($I_2 = 54.4$ eV) are clearly visible.

For pulses of the order of one hundred attoseconds a dramatically different picture emerges: the two peaks merge into a single one located near the point of symmetric energy sharing. It should be noted that this is not simply due to the Fourier broadening of the pulse. Instead, the close proximity in time of the two emission events allows for energy exchange between the two outgoing electrons representing a clear departure from the independent-particle behavior [22, 25]. Differently stated, the time interval between the two ionization events is too short for the “remaining” electron to relax to a stationary ionic state. In the limit of ultrashort pulses the notion of a definite time ordering of emission processes loses its significance, as does the distinction between “sequential” and “nonsequential” ionization.

The attosecond-pulse induced dynamical electron correlation becomes more clearly visible in the joint angular distribution $P(\theta_{12}, \theta_1)$ (Fig. 2), where θ_1 is the polar emission angle of one electron with respect to the polarization axis of the XUV pulse, θ_{12} is the angle between the two electrons, and the energies E_1, E_2 are integrated over. Here and in the following we choose coplanar geometry with $\phi_1 = \phi_2 = 0^\circ$. In the limit of “long” pulses ($T_p = 4.5$ fs), the joint angular distribution approaches the product of two independent Hertz

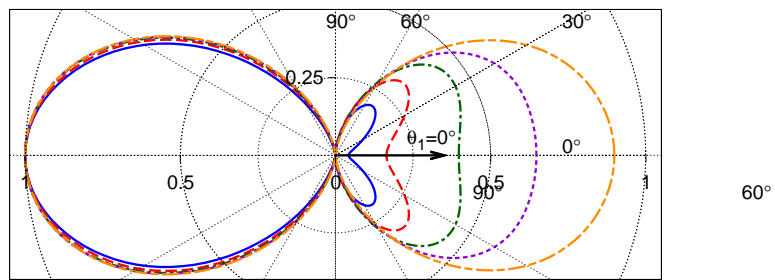


FIG. 2: Conditional angular distributions $P(\theta_{12}, \theta_1 = 0^\circ)$ of the ejected electrons for different pulse lengths at $\hbar\omega = 70$ eV. The innermost (solid blue) line is for $T_p = 75$ as FWHM, with successive lines for $T_p = 150$ as, 300 as, 750 as, and 4500 as FWHM. For better comparison the distributions are normalized to a maximum value of one.

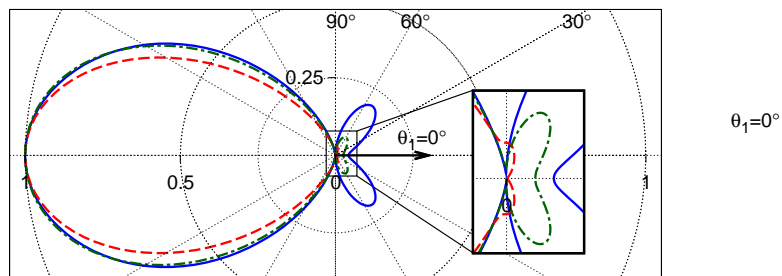


FIG. 3: Conditional angular distributions $P(\theta_{12}, \theta_1 = 0^\circ)$ for a 75 as (FWHM) pulse at $\hbar\omega = 70$ eV (solid blue) and for 2 fs (FWHM) pulses at 42 eV (dashed red) and 52 eV (dash-dotted green). The distribution for the ultrashort pulse strongly resembles the long-pulse distribution in the nonsequential regime ($\hbar\omega < 54.4$ eV).

dipoles, each of which signifies the independent interaction of one electron with one photon. Consequently, also the conditional angular distribution $P(\theta_{12}, \theta_1 = 0^\circ)$ corresponds to a Hertz dipole. With decreasing pulse duration, $P(\theta_{12}, \theta_1 = 0^\circ)$ is strongly modified and develops a pronounced forward-backward asymmetry. The conditional probability for the second electron to be emitted in the same direction as the first is strongly suppressed. It is worth noting that this strong preference for back-to-back emission for $T_p \leq 150$ as persists after integration over the electron energies. Nevertheless, approximately equal energy sharing dominates (cf. Fig. 1). Thus, the dominant break-up mode induced by an attosecond pulse corresponds to the “Wannier ridge” configuration [27]. The same break-up mode is observed in the nonsequential TPDI regime ($\hbar\omega < 54.4$ eV, cf. Fig. 3), where the electrons need to exchange energy to achieve double ionization. Thus, even in long pulses only electrons ionized within a short time of each other can be observed.

It is now instructive to inquire into the origin of the strong angular correlations observed for short pulses. Three different sources can be distinguished:

(i) Correlations in the helium ground state. Due to Coulomb repulsion, the electrons in the ground state are

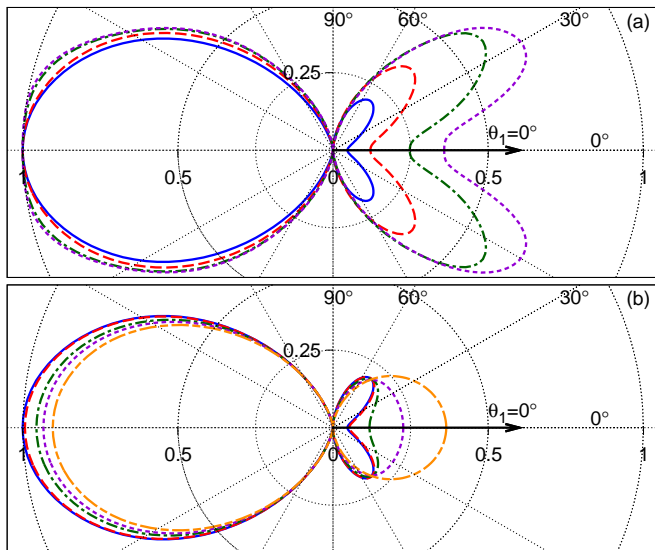


FIG. 4: Conditional angular distributions. (a) For a duration (FWHM) of 75 as for different photon energies. From inside to outside: 70 eV, 91 eV, 140 eV, and 200 eV. The amount of asymmetry decreases with increasing pulse energy. (b) For different observation times after the 75 as FWHM pulse at $\hbar\omega = 70$ eV. Snapshots were taken (from the outermost to the innermost line) immediately at the end of the pulse and 50 as, 150 as, 600 as, and 1000 as after the end of the pulse.

not independent of each other. For ultrashort pulses, TPDI can thus be interpreted as a probe that maps out the initial-state correlations.

(ii) Induced dipole polarization in the intermediate state. When the first electron leaves the core, its electric field induces polarization of the remaining ion, leading to an asymmetric probability distribution of the second electron. The second photon then probes the dynamics in this bound-free complex, such that TPDI can be interpreted as a pump-probe setup.

(iii) Final-state electron-electron interaction in the continuum. After the second electron has been released within the short time interval T_p as well, their mutual repulsion may redirect the electrons.

While the dividing line between those mechanisms is far from sharp, the present time-dependent wave packet propagation allows to shed light on their relative importance since they occur on different time scales. Relaxation of the ground-state correlations (i) is expected to occur on the time scale of the orbital period of the residual electron. As the remaining one-electron wave function will be mostly in the $n = 1$ and $n = 2$ shells, the timescale for this relaxation can be estimated as $t_{(i)} \approx \hbar/(E_2 - E_1) \approx 16$ as, where E_n is the binding energy in the n -th shell of the He^+ ion. Therefore, ground-state correlations will become clearly visible only for pulses with durations shorter than those investigated here. The time scale for induced dipole polarization (ii) can be estimated by the time the first electron takes to escape

to a distance where it does not influence the remaining bound electron strongly. Choosing a somewhat arbitrary distance of 10 a.u., the time necessary for the first electron to reach this distance after absorbing a 70 eV photon is about 120 as and thus of the order of the pulse lengths T_p considered. For higher photon energies, the first electron escapes more quickly, decreasing the importance of this effect. In order to verify this energy dependence, we have performed calculations at various photon energies for $T_p = 75$ as. Fig. 4a demonstrates that for higher energies the asymmetry of the joint angular distribution is indeed strongly reduced.

Long-range Coulomb interactions in the continuum (iii) extend over much longer timescales which strongly depend on the relative emission angles and energies of the electrons, i.e., $|\mathbf{k}_1 - \mathbf{k}_2|$. For example, for two electrons ejected in the same direction and with similar energies, the interaction will last much longer than for ejection in opposite directions. This can be verified by using an ultrashort pulse to start a two-electron wave packet in the continuum and observing the evolution of the joint angular distribution after the laser pulse is switched off (Fig. 4b). Directly after the pulse, the distribution of the electrons shows a decreased probability for ejection on the same side of the nucleus (primarily because of (ii)), but the lobes in forward and backward direction still mostly retain the shape expected from a dipole transition. As time passes, continuum final-state interactions persist and the joint angular distribution develops a pronounced dip at equal ejection angle. The change at larger relative angles is almost negligible.

One remarkable feature of the conditional angular distribution is the persistence of the nodal plane at $\theta = 90^\circ$. While correlation effects strongly perturb the shape of the independent-particle dipolar shape, the nodal plane expected for the angular distribution of two electrons absorbing one photon each is preserved. This is in contrast to one-photon double ionization, where only one electron absorbs the photon energy and electron ejection at angles normal to the polarization axis is indeed observed [7]. On the other hand, the conditional angular distribution in the nonsequential regime also exhibits a nodal plane at $\theta = 90^\circ$ (cf. Fig. 3).

Additional insights can be gained from a projection of the two-electron momentum onto the energy-angle plane,

$$P(E_1, \theta_{12}, \theta_1 = 0^\circ) = \int P(E_1, E_2, \Omega_1, \Omega_2) dE_2, \quad (2)$$

in coplanar geometry and for $\theta_1 = 0^\circ$. While for long pulses the energy of the emitted electrons is independent of the relative emission angle (Fig. 5c), strong energy-angle correlations appear for short ($T_p \leq 450$ as) pulses. The dominant emission channel is the back-to-back emission at equal energy sharing ($E_1 \approx 30$ eV). This corresponds precisely to the well-known Wannier ridge riding mode [27], previously observed in e-2e ionization pro-

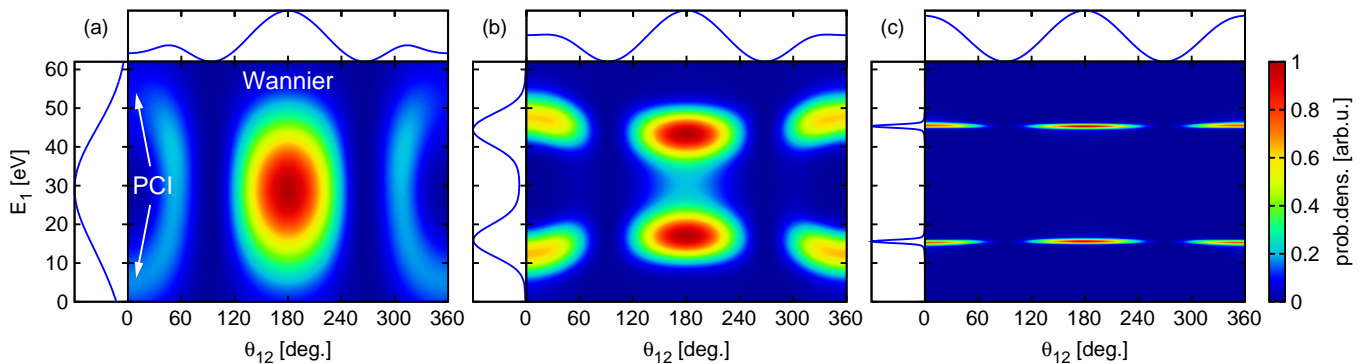


FIG. 5: Angle-energy distribution $P(E_1, \theta_{12}, \theta_1 = 0^\circ)$ in coplanar geometry at 70 eV photon energy for different pulse durations: (a) 150 as, (b) 450 as, (c) 4500 as FWHM. The side plots show the distribution integrated over, respectively, energy and angle.

cesses [28] and also invoked in the classification of doubly-excited resonances [29]. Because of the large instability of the Wannier orbit its presence is more prevalent in breakup processes than in quasi-bound resonances. A second subdominant but equally interesting channel opens for short pulses at $\theta_{12} = 0^\circ$, i.e., emission in the *same* direction. One of the electrons is slowed down while the other one is accelerated. Hence, the slow electron “pushes” the fast electron from behind, transferring part of the energy absorbed from the photon field to the faster electron. This is the well-known *post-collision interaction* [30–32] first observed by Barker and Berry in the decay of autoionizing states excited through ion impact [33].

In conclusion, we have shown that for attosecond XUV pulses the conventional scenario of “sequential” two-photon double ionization (TPDI) breaks down. Due to the small time interval between the two photoabsorption processes dynamical electron-electron correlations can be tuned by the pulse duration T_p . One can view TPDI as an XUV-XUV *pump-probe* process. The angular and angle-energy distributions reveal the signatures of electronic correlation induced by the Coulomb interaction in the intermediate bound-free complex and in the final state with both electrons in the continuum. For short pulses, two well-known scenarios, the Wannier ridge riding mode and the post-collision interaction process, are simultaneously present in the two-electron emission spectrum.

We thank K. Ishikawa for interesting discussions. J.F., S.N., R.P., E.P., and J.B. acknowledge support by the FWF-Austria, Grant No. SFB016. Computational time provided under Institutional Computing at Los Alamos. The Los Alamos National Laboratory is operated by Los Alamos National Security, LLC for the National Nuclear Security Administration of the U.S. Department of Energy under Contract No. DE-AC52-06NA25396.

- [1] M. Hentschel et al., *Nature* **414**, 509 (2001).
- [2] G. Sansone et al., *Science* **314**, 443 (2006).
- [3] E. Goulielmakis et al., *Science* **320**, 1614 (2008).
- [4] J. S. Parker, E. S. Smyth, and K. T. Taylor, *J. Phys. B* **31**, L571 (1998).
- [5] F. W. Byron and C. J. Joachain, *Phys. Rev.* **164**, 1 (1967).
- [6] D. Proulx and R. Shakeshaft, *Phys. Rev. A* **48**, R875 (1993).
- [7] H. Bräuning et al., *J. Phys. B* **31**, 5149 (1998).
- [8] J. S. Briggs and V. Schmidt, *J. Phys. B* **33**, R1 (2000).
- [9] L. Malegat, P. Selles, and A. K. Kazansky, *Phys. Rev. Lett.* **85**, 4450 (2000).
- [10] W. Ackermann et al., *Nat. Photonics* **1**, 336 (2007).
- [11] Y. Nabekawa et al., *Phys. Rev. Lett.* **94**, 043001 (2005).
- [12] B. Dromey et al., *Nat. Phys.* **2**, 456 (2006).
- [13] M. Lein, E. K. U. Gross, and V. Engel, *Phys. Rev. Lett.* **85**, 4707 (2000).
- [14] A. Staudte et al., *Phys. Rev. Lett.* **99**, 263002 (2007).
- [15] A. Rudenko et al., *Phys. Rev. Lett.* **99**, 263003 (2007).
- [16] L. A. A. Nikolopoulos and P. Lambropoulos, *J. Phys. B* **40**, 1347 (2007).
- [17] E. A. Pronin et al., *J. Phys. B* **40**, 3115 (2007).
- [18] D. A. Horner, C. W. McCurdy, and T. N. Rescigno, *Phys. Rev. A* **78**, 043416 (2008).
- [19] J. Feist et al., *Phys. Rev. A* **77**, 043420 (2008).
- [20] P. Antoine et al., *Phys. Rev. A* **78**, 023415 (2008).
- [21] X. Guan, K. Bartschat, and B. I. Schneider, *Phys. Rev. A* **77**, 043421 (2008).
- [22] K. L. Ishikawa and K. Midorikawa, *Phys. Rev. A* **72**, 013407 (2005).
- [23] I. F. Barna, J. Wang, and J. Burgdörfer, *Phys. Rev. A* **73**, 023402 (2006).
- [24] E. Fomouou et al., *New J. Phys.* **10**, 025017 (2008).
- [25] B. Piraux et al., *Eur. Phys. J. D* **26**, 7 (2003).
- [26] J. Ullrich et al., *Rep. Prog. Phys.* **66**, 1463 (2003).
- [27] G. H. Wannier, *Phys. Rev.* **90**, 817 (1953).
- [28] S. Cvejanovic and F. H. Read, *J. Phys. B* **7**, 1841 (1974).
- [29] G. Tanner, K. Richter, and J. M. Rost, *Rev. Mod. Phys.* **72**, 497 (2000).
- [30] G. Gerber, R. Morgenstern, and A. Niehaus, *J. Phys. B* **5**, 1396 (1972).
- [31] A. Russek and W. Mehlhorn, *J. Phys. B* **19**, 911 (1986).
- [32] G. B. Armen et al., *Phys. Rev. A* **36**, 5606 (1987).
- [33] R. B. Barker and H. W. Berry, *Phys. Rev.* **151**, 14 (1966).

* Electronic address: johannes.feist@tuwien.ac.at